Spherical Indentation 실험을 이용한 재료 소성 물성치 측정방법

A Method of Measuring the Plastic Properties of Materials using Spherical Indentation

이 광 하* 강 윤 식** Xi Chen*** 박 대 효†
Li, Guanghe Kang, Yoon-Sik Park, Taehyo

요 지

본 논문에서는 단 한번 만의 간단한 구형 인덴테이션 임프레션 실험을 통하여 재료 소성 물성치를 측정함에 있어서 효율적인 알고리즘이 개발되었다. 본 논문에서는 레프리젠터티브 스트레인의 새로운 정의를 기반으로 연구가 수행되어 예전의 연구와 비교할 때 상당한 량의 피팅 매개변수의 개수를 줄이게 됨으로서 계산 량이 대폭 줄어들면서 연구가 쉽게 진행될 수 있었다. 또한 레프리젠터티브 스트레인에 대한 새로운 정의는 보다 명확한 물리적 임의를 부여하였다.

역 해석의 신뢰성을 증명하기 위하여 본 논문에서는 거의 모든 공학적 금속과 합금이 포함되는 재료 세트들을 사용하여 해석을 진행하였다. 수치 해석 모델링을 통하여 얻은 $P-\delta$ 그래프를 바탕으로 하여 인덴테이션 반응 특성과 재료의 탄소성 물성치가 양 함수에 의하여 연계되었고, 역 해석방법을 적용시켜 재료의 항복응력과 power-law 경화 지수가 얻어진다. 마지막으로, 역 해석을 통하여 얻어진 재료 물성 치와 실제 실험을 통하여 얻어진 재료 물성치가 좋은 일치성을 가진다는 것을 보여준다.

핵심용어 : 구형 인덴테이션, 역 해석방법, 재료 소성치, 유한요소법

Abstract

In this paper, an efficient algorithm is established in order to estimate the plastic properties of power-law hardening bulk specimen materials with one simple spherical indentation impression test. This work is based on a new formulation of representative strain and, therefore, compare to the preceding approaches the fitting parameters are significantly reduced. Moreover, the new definition of representative strain endowed more physical meaning to the representative strain.

In order to verify the reliability of the reverse analysis, we have studied a broad set of materials whose property ranges cover essentially all engineering metals and alloys. Based on the indentation force-displacement $P-\delta$ curves obtained from numerical simulations, the characteristics of the indentation response and material elastoplastic properties are bridged via explicit functions. Next, through the procedure of reverse analysis the yield stress and power-law hardening exponent of bulk specimen materials can be determined. Finally, good agreement between the result from reverse analysis and initial input data from experiment can be observed.

Keywords : *spherical indentation, reverse analysis, plastic property, FEM analysis*

1. Introduction

Instrumented indentation is widely used to probe the elastic and plastic properties of engineering materials, including metals and alloys that are important to structural engineering. During the

† 책임저자, 종신회원 · 한양대학교 건설환경공학과 교수
Tel: 02-2220-0321 ; Fax: 02-2220-4572
E-mail: cepark@hanyang.ac.kr
* 한양대학교 건설환경공학과 석사과정
** 한양대학교 건설환경공학과 박사과정
*** 콜롬비아대학교 지구환경공학과 부교수

• 이 논문에 대한 토론을 2010년 10월 30일까지 본 학회에 보내주시면 2010년 12월호에 그 결과를 게재하겠습니다.

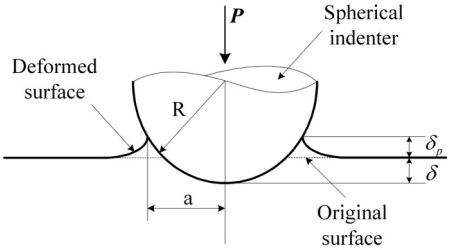

(a) Spherical indentation with bulk specimen

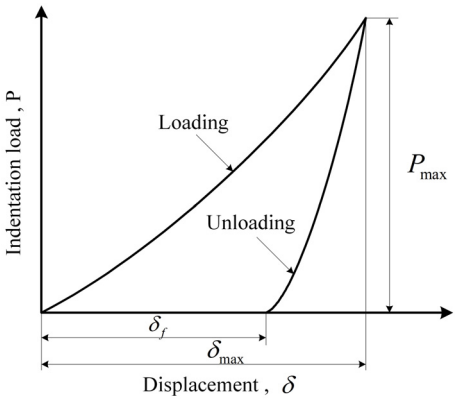

(b) Typical indentation load-depth curves obtained from experiment

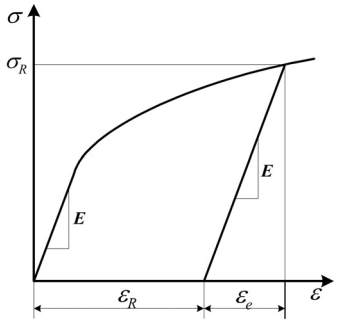

(c) The uniaxial stress-strain curve of materials obeying the power-law hardening law

Fig. 1

experiment, a rigid indenter normally penetrates into a homogeneous solid specimen as shown in the Fig. 1(a), and the indentation load P and displacement δ, are continuously recorded during loading and unloading(since certain aspects such as constant stiffness may be subjected to more prominent measurement error, in this paper, we focus on the loading part while ignore the unloading part) as shown in the Fig. 1(b). Denoting the specimen Young's modulus by E and yield stress by σ_y, without losing generality, the uniaxial stress-strain($\sigma-\varepsilon$) curve of a stress-free solid can be expressed in a power-law form Eq. (1)

$$\sigma = E\varepsilon \text{ for } \varepsilon \le \sigma_y/E \text{ and } \sigma = R\varepsilon^n \text{ for } \varepsilon \ge \sigma_y/E \qquad (1)$$

where n is the work-hardening exponent, for most ductile metals and alloys n is between 0.1 and 0.5. $R \equiv \sigma_y(E/\sigma_y)^n$ is the work-hardening rate. In addition, the Poisson's ratio is usually regarded as a relatively minor factor in this work. Therefore, we fix the value as ν=0.3 for all engineering materials during indentation analysis.

Compared with the commonly used sharp indentation test(e.g. using the Berkovich or Vickers tip), a deep spherical indentation test does not have self-similarity, allowing one to use just one simple impression test to obtain fairly accurate elastic-plastic properties of the bulk specimen. That is, if the sharp indenter is employed, owing to the self-similarity at different indentation depths, one must employ at least two different indenter tips with different apex angle α. In addition to the inconvenience of obtaining two different indenter tips, the impression must be made twice on the same specimen and separated with a practical distance, which makes it impossible to obtain accurate information from one specific point of interest of the material(Zhao et al., 2006). Deep spherical indentation, on the other hand, may deduce elastoplastic properties from just one test and the critical information can be obtained from different depths, thus becoming more practical and efficient(Chen et al., 2005).

2. Background

In this section, we first briefly introduce the background of spherical indentation. There have been several attempts to measure the plastic properties based on the spherical indentation $P-\delta$ curves.

Huber and Tsakmakis(1999) extracted material plastic properties from spherical indentation by using neural network method, which included too many fitting parameters with a relatively complex

algorithm. Ahn and Kwon(2001) obtained plastic properties of bulk specimen by relating the effective strain to the effective stress, this method require high accurate measurement of contact radius(while the indenter is in contact with the specimen). Therefore, the above approaches are less practical in real experiments. If we assume that the elastic modulus is already known using established techniques, the focus will be to determine the plastic material properties of bulk specimen. Cao and Lu(2004) applied the concept of representative strain from conical indentation(Dao et al., 2001) to the spherical indentation with two very shallow indenter depths. However, their dimensionless fitting function was only valid for $\overline{E}/\sigma_R(\varepsilon_R)<200$, which makes its application too limited, in other words, this method is inapplicable for large range of engineering materials (Zhao et al., 2006). Cao et al.(2007) improved their definition of the representative strain in a later paper. However, the formulation still involved too many fitting parameters, and it also required advanced numerical analysis(Ogasawara et al., 2009). In addition, an eminent disadvantage of the preceding shallow spherical indentation studies(Huber and Tsakmakis, 1999; Cao and Lu, 2004; Cao et al., 2007) is that they may not lead to unique solution (Chen et al., 2007). Moreover, indentation experiment with shallow indenter depth may interact with the strain gradient effect and make it difficult to measure the plastic material properties(Ogasawara et al., 2009).

In this paper, the spherical indentation experiment is carried out with sufficient deep depth $\delta_{\max}/R=0.3$, in order to avoid the effect of strain gradient and non-uniqueness. In addition, the new definition of representative strain(Zhao et al., 2006) is applied to reduce the number of fitting parameters to minimum. Moreover, a wide range of materials whose property ranges cover essentially all engineering metals and alloys are used to verify the reliability of reverse analysis. Furthermore, assuming the elastic modulus of this materials are already known, in order to, make this work execute simpler than the preceding approaches.

3. Dimensional analysis

Based on the new definition of representative strain(Zhao et al., 2006), the representative strain is defined to be the plastic strain, for uniaxial loading as shown in Fig. 1(c):

$$\varepsilon=\varepsilon_e+\varepsilon_P\equiv\varepsilon_e+\varepsilon_R \tag{2}$$

The representative strain ε_R is a function of δ/R. In order to do this, close to that of the Berkovich indenter and cube indenter, we choose two indentation depths $\delta_1/R=0.13$ and $\delta_2/R=0.3$ respectively(Dao et al., 2001). These values are adequately deep to overcome the strain gradient effect(Ogasawara et al., 2005) as well as ensuring uniqueness of indentation analysis(Chen et al., 2007).

Correspondingly, the representative stress is:

$$\sigma_R(\varepsilon_R)=\sigma_y[\frac{E}{\sigma_y}(\frac{\sigma_R(\varepsilon_R)}{E}+\varepsilon_R)]^n \tag{3}$$

Dimensional analysis leads to:

$$\frac{C_1}{\sigma_R^{(1)}(\varepsilon_R^{(1)})}\equiv\frac{P_1}{\delta_1^2\sigma_R^{(1)}(\varepsilon_R^{(1)})}=\Pi_1(\frac{\overline{E}}{\sigma_R^{(1)}(\varepsilon_R^{(1)})},n) \tag{4}$$

and

$$\frac{C_2}{\sigma_R^{(2)}(\varepsilon_R^{(2)})}\equiv\frac{P_2}{\delta_2^2\sigma_R^{(2)}(\varepsilon_R^{(2)})}=\Pi_2(\frac{\overline{E}}{\sigma_R^{(2)}(\varepsilon_R^{(2)})},n) \tag{5}$$

where, P_1 and P_2 are the indentation loads measured at $\delta_1/R=0.13$ and $\delta_2/R=0.3$ respectively, $\varepsilon_R^{(1)}$ and $\varepsilon_R^{(2)}$ are the representative strains corresponding with $\delta_1/R=0.13$ and $\delta_2/R=0.3$ respectively. Where, $\overline{E}=E/(1-\nu^2)$ is the plane strain modulus. The dimensionless functional forms will be determined by fitting the numerical results via extensive forward analysis. In this paper, we assume that the value of E is already known(can be determined via well-established techniques, e.g. Oliver and Pharr(1992)

and Fisher-Cripps(2001). Therefore, the plastic material properties(σ_y, n) can be determined from simultaneous equations (4) and (5).

4. Forward analysis

4.1 Load-displacement curves of spherical indentation

In this paper, the finite element simulations were performed by using ABAQUS(6.9-1). The indenter is assumed rigid and the specimen is semi-infinite(Fig. 2 and Fig. 3). In this work the radius of spherical indenter setup as R=0.0012mm(all results are normalized such that the specific value of indenter radius does not matter), the friction coefficient was taken to be 0.1 and as mentioned before, the Poisson's ratio fixed as 0.3; both are relatively minor factors during indentation analysis.

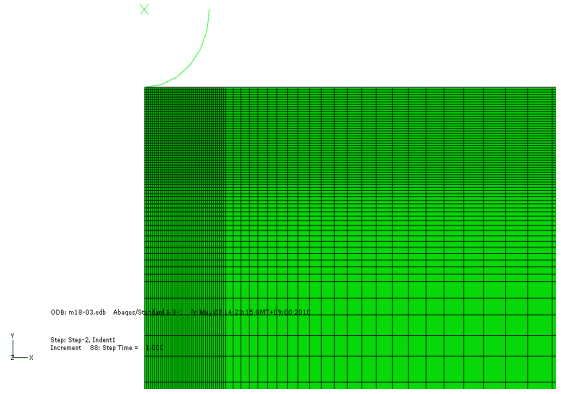

Fig. 2 ABAQUS(6.9.1) modeling-Mesh

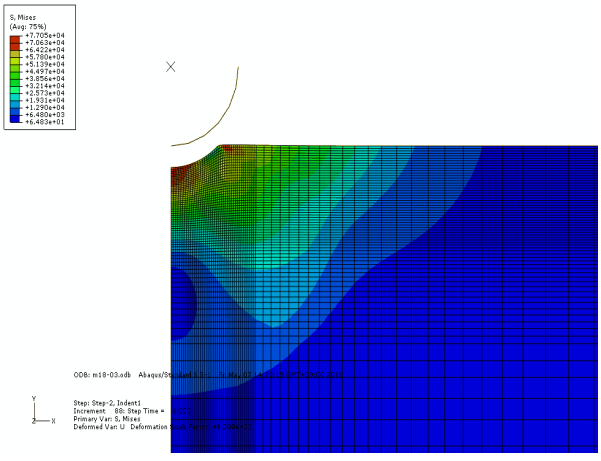

Fig. 3 ABAQUS(6.9.1) modeling-Deformation

Fig. 2 shows that the numerical model built in an axisymmetric space. Moreover, the mesh of bulk specimen that below the spherical indenter part was refined for obtaining rather smooth load-displacement curves.

Fig. 3 shows that the bulk material specimen was deformed due to the effect of spherical indentation that was normally impressed on the surface. As mentioned before, the spherical indenter was modeled as a rigid body, therefore, the Fig. 3 presents the material specimen deformation after the impression force from spherical indenter was removed.

In the forward analysis, the parameters are varied over a large range to cover essentially all engineering metals and alloys, with $\overline{E}/\sigma_R$ from 3 to 3500 and n from 0.1 to 0.5.

As mentioned before, owing to the values of elastic modulus are already known, therefore, only the loading curves are needed for measuring the plastic parameters in this paper.

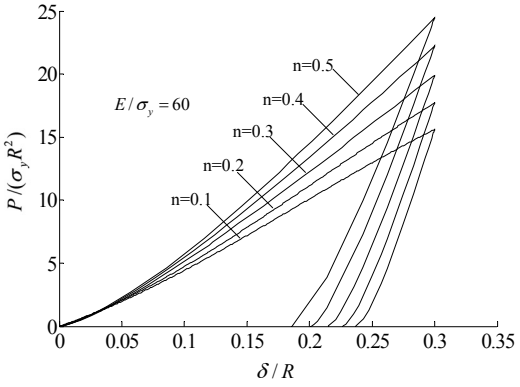

Fig. 4 $E/\sigma_y = 60$ with varying n

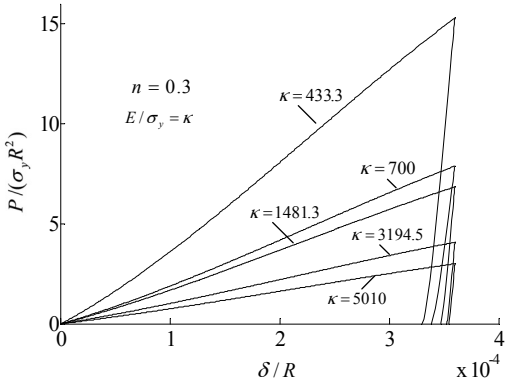

Fig. 5 n=0.3 with varying E/σ_y

Representative load-displacement curves are obtained from FEM analysis are given in Fig. 4 and Fig.5. The Fig. 4 shows the cases for E/σ_R=60 with different $n$and the Fig. 5 shows that the load-displacement curves for n=0.3 with different values of E/σ_R. From above two figures we can understand that the values of n have certain effects to the results.

4.2 The dimensionless functions

Based on the equations (4) and (5), adjusting the representative stress-strain values and using the least squares method, the best fitting functions (6)-(11) can be obtained for δ_1/R=0.13, $\varepsilon_R^{(1)}$ = 0.0374, and for δ_2/R=0.3, $\varepsilon_R^{(2)}$ =0.0674 respectively. Owing to the self-similarities of the relationships between $C/\sigma_R(\varepsilon_R)$ and $\overline{E}/\sigma_R(\varepsilon_R)$, good fittings of Π_1 and Π_2 can still be obtained by separating the variables:

$$\Pi_1\left(\frac{\overline{E}}{\sigma_R^{(1)}(\varepsilon_R^{(1)})},n\right)=\Pi_1(m_1,n)=H_1(m_1)\times K_1(n) \qquad (6)$$

Where, $m_1=\dfrac{\overline{E}}{\sigma_R^{(1)}(\varepsilon_R^{(1)})}$

$$\Pi_2\left(\frac{\overline{E}}{\sigma_R^{(2)}(\varepsilon_R^{(2)})},n\right)=\Pi_2(m_2,n)=H_2(m_2)\times K_2(n) \qquad (7)$$

Where, $m_2=\dfrac{\overline{E}}{\sigma_R^{(2)}(\varepsilon_R^{(2)})}$

$$H_1(m_1)=62.9-85.51\times\ln(m_1)+48.5\times(\ln(m_1))^2 -6.79\times(\ln(m_1))^3+0.299\times(\ln(m_1))^4 \qquad (8)$$

$$K_1(n)=0.747+0.022\times n-0.113\times n^2-0.19\times n^3 \qquad (9)$$

$$H_2(m_2)=44.15-56.61\times\ln(m_2)+52.77\times(\ln(m_2))^2 -8.65\times(\ln(m_2))^3+0.43\times(\ln(m_4))^4 \qquad (10)$$

$$K_2(n)=0.203+0.018\times n-0.577\times n^2+0.461\times n^3 \qquad (11)$$

The numerical results of the best fitted dimensionless functions Π_1 and Π_2 are given in Fig. (6) and Fig. (7) respectively. It can be seen that when

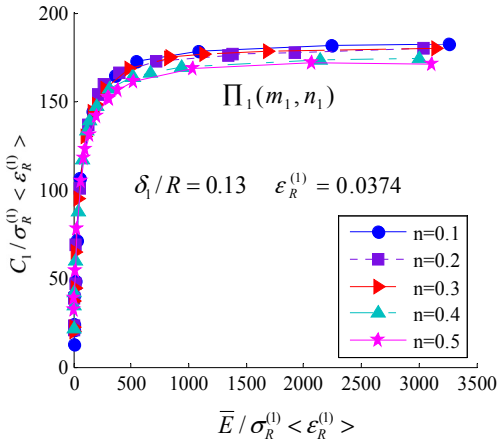

Fig. 6 Dimensionless function Π_1

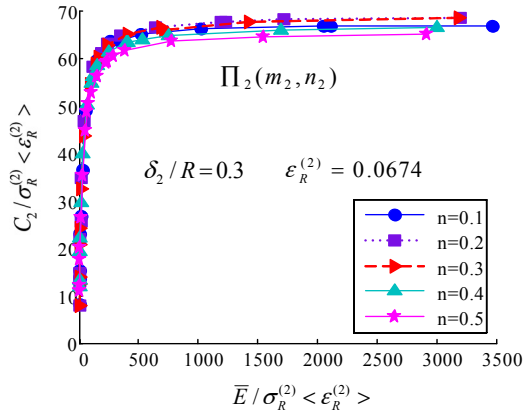

Fig. 7 Dimensionless function Π_2

$\overline{E}/\sigma_R(\varepsilon_R)$ is kept in the same range, the values of $\dfrac{C_1}{\sigma_R^{(1)}(\varepsilon_R^{(1)})}$ and $\dfrac{C_2}{\sigma_R^{(2)}(\varepsilon_R^{(2)})}$ depend on both variables $\overline{E}/\sigma_R(\varepsilon_R)$ and n, although the dependence on n is less obvious.

5. Reverse analysis

5.1 The introduction of reverse analysis

In the reverse analysis(Zhao et al., 2006), the parameters of C_1 and C_2 can be measured from results of ABAQUS(6.9-1) simulations with $\delta_{\max}/R$= 0.3. Note that the indentation test does not have to have a maximum indentation depth of 30% the indenter radius - as long as the maximum depth is beyond $0.3R$, the corresponding normalized load taken from δ_1/R=0.13 and δ_2/R=0.3 can be

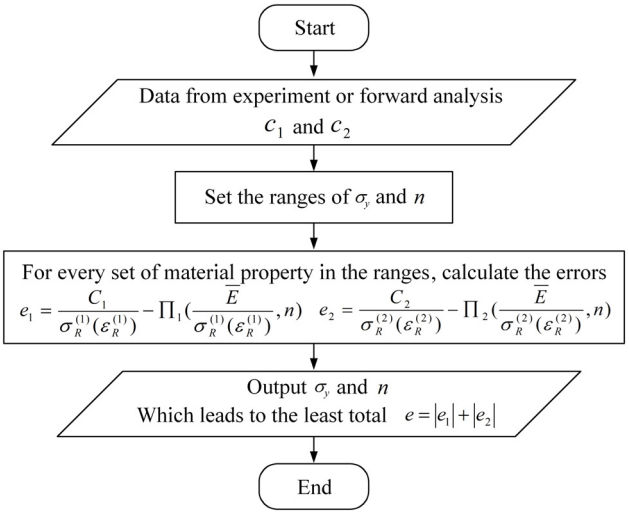

Fig. 8 The flow chart of reverse analysis

employed. From equation (4) and (5), the relationship between parameter C and $P-\delta$ can be derived and can be written as $C_1 = \frac{P_1}{\delta_1^2}$ and $C_2 = \frac{P_2}{\delta_2^2}$ respectively. Next, for initially guessed ranges of σ_y and n based on equations (4) and (5), through the optimization method, the values of e_1 and e_2 can be determined respectively. In other words, when the value of $|e_1|+|e_2|$ is the least, the corresponding values of plastic properties(σ_y, n) are the target values to be find out. The procedures of reverse analysis are shown as the flow chart in Fig. 8. A final validation can be carried out via equations (4) and (5) to make sure that the identified solution is the global minimum of the nonlinear functions.

5.2 Numerical examples of reverse analysis

In order to estimate the effectiveness of reverse analysis algorithm, numerical indentation tests are applied firstly. A large range of different material combinations(σ_y, n) are used as the input data in FEM simulations and the resulting load-displacement data are then employed to calculate indentation parameters C_1 and C_2. The example of numerical analysis is shown in Table 1.

The input material properties are compared with those identified from reverse analysis. Note that none of these parametric combinations were used in generating Eqs. (6)~(11). From Table 1, all reverse analysis results are fairly accurate with error less than 10%.

5.3 Comparison with real experiments in the literature

Next, we examine the performance of the current approach with experimental result available in literature. Taljat et al. carried out spherical indentation experiments with cold-worked copper and A533-B steel. Both of the metals have $\delta_{\max}/R$ values close to 0.3 in their experiment. Therefore, we can use the experimental data to demonstrate the effectiveness of reverse analysis well in this paper. In Fig. 9 the solid lines represent the experimental data that are obtained by uniaxial compression tests as the reference properties(Taljat et al., 1998) and the dash lines represent the model by power-law hardening equations (use the equation.(1)). The fitted power-law properties of materials are E=117GPa, σ_y=338MPa and n=0 for cold-worked copper and E=210GPa, σ_y=400MPa and n=0.127 for A533-B steel. In Fig. 10 the solid line and dash line represent the experiments $P-\delta$ curves for A533-B steel and cold-worked-copper respectively, the solid symbols represent the forward analysis(numerical analysis) and the open symbols represent the reverse analysis.

During the forward analysis, we put E=117GPa, σ_y=338MPa and n=0 for cold-worked copper and E=210GPa, σ_y=400MPa and n=0.127 for A533-B steel into the FEM simulation and then, the $P-\delta$ curves can be obtained. The reverse analysis, on the other hand, is based on the experimental $P-\delta$ curves, and after the material properties are determined via optimization as shown in the Figure 8, a numerical indentation test is carried out to obtain the hollow symbols in Figure 10. From the Fig. 10 we can observe that the $P-\delta$ curves of forward analysis and reverse analysis are really close, but both of them have a little bit of difference with real experiment $P-\delta$ curve, especially into the plastic area. This is because the real material does not satisfy the

Table 1. Comparison between the identified material properties from reverse analysis and input material properties

		Input properties		Identified plastic properties by reverse analysis	
	E(GPa)	σ_y(MPa)	n	σ_y(MPa)	n
Brass	96	843	0.36	850	0.35
Au	82	286	0.25	276.89	0.233
Al	70	159	0.295	171.03	0.283
Steel	210	500	0.1	507.4	0.097

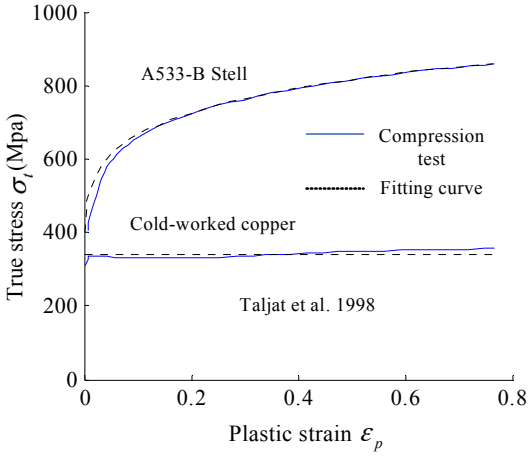

Fig. 9 Comparison between the uniaxial compression test and modeled by power-law stress-plastic strain curves

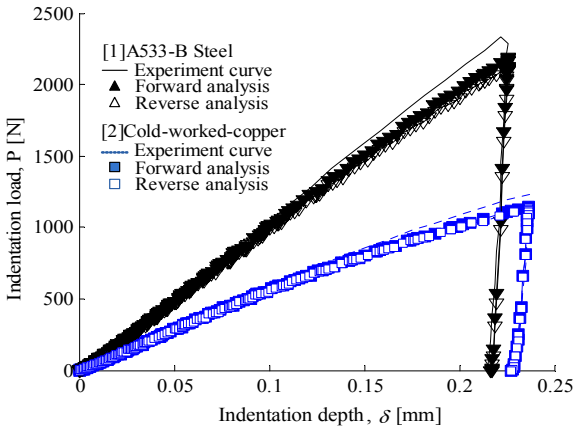

Fig. 10 Comparison between experiment, power-law forward analysis and reverse analysis

power-law hardening equation exactly. Through the forward analysis, the indentation parameters C_1 and C_2 are determined from the numerical $P-\delta$ curves, and then put these parameters into the reverse analysis algorithm to solve(σ_y, n). Finally, the material behavior can be obtained from reverse analysis. Fig. 10 shows that the reverse analysis and the forward analysis are agreed very well.

6. Conclusion

Spherical indentation has potential for measuring the elastoplastic properties of bulk materials by just using one simple impression test, and it works well for a large range of materials(almost cover all engineering materials).

In this paper, owing to the analysis based on the new definition of representative strain(Zhao et al., 2006), therefore, reduces the number of unknown parameters. Moreover, assume the values of elastic modulus of materials are already known. For these reasons, this analysis executed much simpler than preceding approaches.

Reverse analysis established in this paper proves to be a practical, simple and fairly accurate way for determining the plastic properties of materials. For the wide range of material properties investigated in this paper, the error between reverse analysis result and original input data less than 10% in most cases, and the algorithm is also validated by comparing with experimental data in literature. Therefore, the reverse analysis has fair accuracy for measuring the material properties.

Acknowledgement

This research was supported by WCU(World Class University) program through the National Research Foundation of Korea funded by the Ministry of Education, Science and Technology(R32-2008-000-20042-0).

Reference

ABAQUS 6.9-1 user's manual.

Ahn, J.H., Kwon, D. (2001) Derivation of Plastic Stress-Strain Relationship from Ball Indentations: Examination of Strain Definition and Pileup Effect, *Materials Research Society*, 16(11), pp.3170~3178.

Cao, Y.P., Lu, J. (2004) A New Method to Extract the Plastic Properties of Metal Materials from an Instrumented Spherical Indentation Loading Curve, *Acta Materialia,* 52(13), pp.4023~4032.

Cao, Y.P., Qian, X., Huber, N. (2007) Spherical Indentation Into Elastoplastic Materials: Indentation-Response Based Definitions of the Representative Strain, *Materials Science and Engineering: A,* 454-455, pp.1~13.

Chen, X., Hutchinson, J.W., Evans, A.G. (2005) The Mechanics of Indentation Induced Lateral Cracking, *Journal of the American Ceramic Society*, 88(5), pp.1233~1238.

Chen, X., Ogasawara, N., Zhao, M., Chiba, N. (2007) On the Uniqueness of Measuring Elastoplastic Properties from Indentation: the Indistinguishable Mystical Materials, *Journal of the Mechanics and Physics of Solids,* 55(8), pp.1618~1660.

Dao, M., Chollacoop, N., Van Vliet, K.J., Venkatesh, T.A., Suresh, S. (2001) Computational Modeling of the Forward and Reverse Problems in Instrumented Sharp Indentation, *Acta Materialia*, 49(19), pp.3899~3918.

Fischer-Cripps, A.C. (2001) Use of Combined Elastic Modulus in the Analysis of Depth-Sensing Indentation Data, *Materials Research Society*, 16(11), pp.3050~3052.

Fleck, N.A., Hutchinson, J.W. (1997) Strain Gradient Plasticity, *Advances in Applied Mechanics,* 33, pp.295.

Huber, N., Tsakmakis, Ch. (1999) Determination of Constitutive Properties from Spherical Indentation Data Using Neural Networks. Part I: the case of pure kinematic hardening in plasticity laws, *Journal of the Mechanics and Physics of Solids,* 47(7), pp.1569~1588.

Ogasawara, N., Chiba, N., Chen, X. (2005) Representative Strain of Indentation Analysis. *Materials Research Society,* 20(8), pp.2225~2234.

Ogasawara, N., Chiba, N., Chen, X. (2006) Limit Analysis-Based Approach to Determine the Material Plastic Properties with Conical Indentation, *Materials Research Society*, 21(4), pp.947~957.

Ogasawara, N., Chiba, N., Chen, X. (2009) A Simple Framework of Spherical Indentation for Measuring Elastoplastic Properties, *Mechanics of Materials*, 41(9), pp.1025~1033.

Ogasawara, N., Chiba, N., Zhao, M., Chen, X. (2007) Measuring Material Plastic Properties with Optimized Representative Strain-based Indentation Technique, *Journal of Solid Mechanics and Materials Engineering*, 1(7), pp.895~906.

Oliver, W.C., Pharr, G.M. (1992) An Improved Technique for Determining Hardness and Elastic-Modulus Using Load and Displacement Sensing Indentation Experiments, *Materials Research Society*, 7(6), pp.1564~1583.

Taljat, B., Zacharia, T., Kosel, F. (1998) New Analytical Procedure to Determine Stress-Strain Curve from Spherical Indentation Data, *International Journal of Solids and Structures*, 35(33), pp.4411~4426.

Zhao, M., Ogasawara, N., Chiba, N., Chen, X. (2006) A New Approach to Measure the Elastic-Plastic Properties of Bulk Materials Using Spherical Indentation, *Acta Materialia,* 54(1), pp.23~32.

● 논문접수일 2010년 5월 28일
● 논문심사일
1차 2010년 6월 16일
2차 2010년 8월 5일
● 게재확정일 2010년 8월 10일